Sequential phreatomagmatic eruptions during the lateral propagation of giant dyke swarms

Evan Pryce, Joe Cartwright, Chris Kirkham and Daniel Phillips

Department of Earth Sciences, University of Oxford, South Parks Road, Oxford OX1 3AN, UK

ABSTRACT

Giant dyke swarms are widely developed on Earth, Venus and Mars and form by lateral propagation of constituent dykes over 100s to 1000s of kilometres. The failure of these dykes to erupt magma at surface partly accounts for their long-range propagation. However, the lack of preservation of the upper regions of most terrestrial dykes is a barrier to fully explaining the reasons for this upward arrest below ground level. Here we use 3D seismic and well data to document the near surface expression of dykes comprising the Mull Dyke Swarm from the southern North Sea (UK). The upper tips of these dykes are overlain by linear arrays of craters with deeply eroded bases. Craters are flanked by a tephra apron comprising reworked chalky sediments. The well data allow us to exclude crater forming mechanisms based on collapse into a void, but are consistent with those linked to phreatomagmatic eruption. We propose that the rapid cooling of dyke magma during the phreatomagmatic eruptive process was an important contributory factor in the upward arrest of dyke propagation, preventing surface extrusion and hence promoting lateral propagation.

INTRODUCTION

Giant dyke swarms are capable of transporting huge volumes of magma vertically and laterally over large distances with perhaps the largest effusion rates in the geological record (Fialko and Rubin, 1999). Giant dyke swarms are developed widely on Earth and are also inferred to occur widely on Venus and Mars (Head et al. 1992; Ernst et al. 1995; Scott et al. 2002). Despite intense research, some key aspects of the emplacement of giant dyke swarms remain enigmatic, notably how and why individual dykes in the swarms are able to propagate laterally for 100s to 1000s km without magma erupting at surface (Parfitt and Head, 1993; Ernst et al. 1995; Rivalta et al. 2015).

On Earth, most dykes are highly eroded such that their upper tip regions are no longer preserved, and this inhibits our understanding the factors controlling lateral propagation.

In the past decade or so there have been significant advances in our understanding of magmatic plumbing systems using seismic data (Magee et al. 2019). Of the few seismic-based studies of dykes to date, two have documented the near surface structures associated with long-range lateral propagation of giant dyke swarms, both of which linked their lateral propagation to the development of linearly aligned arrays of small craters (termed pit crater chains) positioned directly above the upper dyke tips (Wall et al. 2010; Magee et al. 2022). However, in neither case was the seismic interpretation of the craters directly calibrated by wells, hence their specific mode of origin is uncertain (see Okubo and Martel (1998) and Wyrick et al. (2004) for detailed discussion).

In this paper, we use a combination of 3D seismic and well data to calibrate the stratigraphic and structural relationships of a >150km long array of craters formed above major constituent dykes of the Mull Dyke Swarm (Carver et al. 2023)(Fig. 1). This dyke swarm traverses mainland Britain to cross into the Southern North Sea Basin (SNSB) where dyke tip structures are preserved intact under a sedimentary cover. Our main aim is to analyse processes in the upper tip regions of laterally propagating dykes by focusing our analysis on the origins of the craters linked to the Mull Dyke Swarm. Critically, one of the wells we analysed was found to transect a crater and its fill. This unique calibration provides an opportunity to constrain the upper tip processes more rigorously than previously possible, with concomitant implications for wider understanding of long-range lateral propagation of giant dyke swarms in general.

STUDY AREA, DATABASE AND METHODS

Our study area in the SNSB (Fig. 1) is based on a large 3D seismic survey tied to > 300 exploration wells previously used to map the Mull Dyke Swarm across the basin. This swarm comprises three major dyke groups that transect major crustal-scale fault zones and sedimentary basins of different ages (Fig. 1A). Onshore, dykes are typically 5-20m wide and are exposed at progressively shallower stratigraphic levels eastwards due to the westerly uplift of Britain post-emplacement at c. 58Ma BP (Carver et al. 2023 and references therein). Dyke heights are unknown but have been estimated at 10km (Macdonald et al. 1988). In the SNSB, they transect the full sedimentary basin succession up to and including the Late Cretaceous Chalk Group, and their upper tip regions are fully preserved over a lateral distance of >250km.

Previous studies have mapped the dykes from their associated 'Seismic Disturbance Zones' (SDZs) (Underhill, 2009; Carver et al. 2023) (Fig. 2; see Supplemental Material[1] Fig. S1). SDZs are attributed to wave scattering and attenuation caused by velocity anomalies and complex dips associated with overlying craters hosted within the uppermost Chalk Group (Brown et al. 1994). In this study, seismic interpretation of craters followed the diagnostic criteria of Wall et al. (2010) and Carver et al. (2023) (see Supplemental Material (SM) for details). Several previously undescribed wells form the main focus of our analysis of the crater forming mechanism as described below 1.Supplemental Material: Background, Methods and Data.

3. RESULTS

Seismic characteristics of the Craters

142 individual craters have been mapped in the study area aligned along three major component dykes of the Mull Dyke Swarm (Fig. 1; Fig. S2). Isolated craters show circular to elliptical planforms, coalescing to form narrow linear troughs with scalloped margins (c.f. Wyrick et al. 2004)(Fig. 2; Fig. S2). Arcuate scarps define many of the lateral margins of craters (Fig. S3). The scalloped margins are systematically asymmetric in the ESE propagation direction of the dykes (Fig. 2B). This pattern of scalloped margins may therefore be useful more widely as a novel kinematic indicator for dyke propagation.

In profile, craters are characterised by a depression at the Top Chalk Horizon (TCH) with a sharply defined margin, and a concave geometry (Fig. 2A). Reflections above the TCH are commonly observed to onlap the crater flanks in a parallel configuration suggestive of passive fill. The TCH within craters is erosional, with clear truncation of intra-Chalk reflections (Fig. 2; Fig. S3). Deeper reflections within the Chalk Group pass beneath craters with no deflection or offset.

The alignment of the craters is close to linear for much of the length of the crater array and crater bases overlie the shallowest part of the SDZs. Where dyke-induced graben are present along strike (only c. 20% of strike length), the craters occur midway between the bounding faults, similar to the relationship mapped by Bosworth et al. (2015) and Magee et al. (2022)(see SM for details). The upper tip positions of dykes are interpreted to lie at a depth range of 200-400m (+/-100m) beneath crater bases based on (1) the geometry of dyke-induced graben faulting (c.f. Magee et al. 2022)(see SM for details), (2) modelling of high-resolution aeromagnetic data (Brown et al. 1994), and (3) upper limits of SDZ for inclined dykes (Fig. S1C) (Carver et al. 2023).

Crater morphometrics measured for a subset in the study area (Fig. S5) show an order of magnitude range in diameter (150-1620m) and relief (10-147m). There is no positive correlation between diameter and spacing or relief and spacing, but a weak one between relief and diameter (Fig. S5).

A prominent amplitude anomaly is identified and mapped along large portions of the strike length of the major dykes in the central group. The amplitude anomalies are restricted to a region within 1-2km of the crater flanks and only occur where there are craters above the dykes (Fig. 3; Figs. S6 and 7). These crater flank anomalies (CFAs) are acoustically positive, range in length from 5km to 50km, and occur intermittently over the entire strike length of the crater arrays.

Well Calibration of Craters and CFAs

Of the several hundred wells drilled for deeper targets (pre-Mesozoic) within the study area, only one well directly transects a crater (well 44/11-3) (Fig. 1B), penetrating a large crater associated with Dyke C (Fig. 3A). Three others provide direct calibration of the CFAs (44/23a-12 (Fig. S7); 44/24-4, and 44/29b-4).

The crater fill drilled by 44/11-3 is recorded in drill cuttings and wireline logs (Fig. 3A). It comprises c. 100m of tuffaceous claystones, a 10m thick interval consisting mainly of tuffs (informally named the Ash Marker), a 15m thick chalky limestone, and a 50m thick mudstone unit. There is no record of the Ash Marker in any of the nearby wells, only minor tuffaceous laminae dispersed within the overlying mudstones assigned to the Balder Formation (Lott and Knox, 1994). The crater fill units exhibit a range of dips (4-26^{o}) contrasting markedly with systematic low dips (<5^{o})

recorded over a similar depth range in nearby wells. The markedly erosive crater base reflection ties at the precise contact between tuffaceous claystones (Late Palaeocene) with chalks of Early Maastrichtian age, implying a considerable missing section. A comparison of Chalk Group thickness with nearby wells (Fig. S8) shows that >200m of upper Chalk Group sediments were removed to form this crater.

The three wells calibrating the CFAs show that the anomalous reflection above the TCH correlates to one or two closely spaced thin (<5m) chalky limestone layers interbedded with mudstones of Mid-Late Palaeocene age. Crucially, the thin chalky limestones contain the diagnostic species *Stensiocoeina pommerana* which is restricted to the Late Maastrichtian, implying that these thin layers are stratigraphically out of place. In all three wells the TCH is dated as Late Maastrichtian (Fig. S7) and is an unconformity surface overlain by mudstones dated as Thanetian (mid Palaeocene) from the occurrence of diagnostic foraminifera such as *Nodosaria torsicostata* indicating a biozone of TM6 (Gradstein et al. 2012).

DISCUSSION

The alignment of the craters along three major dykes of the Mull Dyke Swarm together with their locus <500m above the upper tip positions of the dykes strongly suggests that their genesis is directly connected to the upward arrest of the dyke tips below the contemporaneous surface. The central question for this discussion is to assess what the new observations presented here imply for this genetic mechanism, and how might these contribute to the open questions about long-range dyke propagation?

A range of specific mechanisms have been advocated for the formation of craters above upper dyke tips. These fall into two broad groups: (1) void collapse mechanisms or (2) eruptive mechanisms. The first group include stoping above dyke induced fractures (Okubo and Martel (1998), volatile release leading to near surface collapse (Scott and Wilson, 2002; Wall et al. 2010) and post-emplacement magma withdrawal and collapse (Bosworth et al. 2015; Magee et al. 2022). The second group are either linked to groundwater interaction with the dyke magma leading to phreatomagmatic activity (Lorenz, 1986; Mège and Masson, 1996) or to the involvement of juvenile volatiles in the eruptive process which in some cases lead to Plinian-style eruptions (Scott and Wilson, 2002).

We consider it extremely unlikely that the craters along the Mull Dyke Swarm formed by any mechanism dominated by collapse of surficial material into a void for two main reasons. Firstly, the continuity of reflections underlying the craters within the basal 200m of the Chalk Group (Fig. 2) means that any collapse could only be superficial and confined to within 100-200m of the crater bases. Secondly, the crater bases imaged by the 3D seismic data are strongly erosional, with truncation geometries implying removal (excavation) of over 200m of Chalk Group sediments in some cases (Fig. S8). A collapse mechanism would not remove material, but remould it as it moved structurally downwards to fill a void space (c.f. Wyrick et al. 2004). Additionally, our observations of (a) steeper dips within the crater fill in 44/11-3 and (b) arcuate scarps on many crater margins (e.g. Fig. 2B; Fig. S3) are equally as explicable by minor local collapse during the crater widening process as by collapse into a void at depth.

In a previous study of the craters along a c. 30km long segment of the Mull Dyke Swarm, Wall et al. (2010) argued that they could have formed either phreatomagmatically (invoking the maar-diatreme model of Lorenz,1986) or by escape of juvenile volatiles from the dyke tip (c.f. Scott and Wilson, 2002). However, they were unable to specify the specific driving mechanism or the source of the volatiles involved in the eruptive process because they had no direct evidence of this from any borehole data, nor were they able to identify the necessary tephra apron that is intrinsic to the maar-diatreme model.

Based on our new well calibration of the craters and CFAs, we propose that a phreatomagmatic eruptive mechanism best fits the evidence from the craters in the study area (Fig. 4). Three observations are critical. Firstly, a local derivation best explains the thick development of tuffs in the crater fill (Fig. 3). This Ash Marker unit is much thicker than any of the thin tuff bearing intervals of the Balder Formation drilled in surrounding areas (Morton and Knox, 1990) known to be long distance ash fall from hydromagmatic eruptions along the nascent Atlantic margin (Stokke et al. 2020). Secondly, the close association of CFAs with the craters (Figs. S6 and 7) for >150km along strike strongly argues that the CFAs represent a tephra apron composed from the uppermost Chalk Group sediments that were removed during crater formation (Fig. 4). CFAs cannot be explained by a collapse mechanism, but would be expected in any eruptive mechanism where magma fragmentation combined with explosive expansion of gas phases was involved (Lorenz, 1986; 2003).

Finally, the erosional excavation of the craters themselves (Fig. 2; Fig. S3) matches the predictions of the maar-diatreme model of Lorenz (1986) in which a crater forms directly above the upper tip of the dyke (Fig. 4). Removal of >200m of chalky sediments is best explained by a vigorous eruption. High pressure venting of supercritical steam generated by magmatic flash heating of pore water in the Chalk Group would be capable of such deep excavation (Delaney, 1982). Volcaniclastic debris mixed with excavated chalky sediments would be blasted upwards into the water column, with some of this material settling out to form tephra aprons. Dyke cooling and pore pressure deflation would have led to localised compaction and subsidence of brecciated sediments beneath the crater along with crater widening by failure of crater flank deposits (Fig. 4).

The rapid cooling and fragmentation of the magma in the upper dyke tips involved in a phreatomagmatic eruption would likely have had profound consequences for dyke propagation and may have been a crucial factor in the upward arrest of the dykes below the surface and the prevention of surface eruption of magma (Lorenz, 1986). We cannot infer if the craters originally formed along the entire 650 km lateral extent of the Mull Dyke Swarm since the upper tips are only preserved for the most distal 250 km. However, their ubiquitous development wherever the upper tips entered porous sedimentary layers points to an important but as yet unquantified role for rapid cooling in upward dyke arrest. Other factors may be primarily responsible for upward arrest, such as the loss of buoyancy drive, or magma pressure losses due to narrowing of dyke aperture (Lister and Kerr, 1991; Fialko and Rubin, 1999). However, if phreatomagmatic craters are proven to occur more widely above giant dyke swarms elsewhere, as with the Mull Dyke Swarm, then near surface cooling through groundwater/magma interactions may warrant more serious consideration as a prime control on long-range lateral propagation.

CONCLUSIONS

15okm long, linear arrays of craters formed in the Late Palaeocene in the Southern North Sea Basin are linked to the Mull Dyke Swarm. The strongly erosive crater morphology implies that their genesis involved a powerful erosive process incompatible with a collapse mechanism. Thick tuffs comprising the crater fill combined with reworked chalks in a newly mapped tephra apron flanking the craters best fit a phreatomagmatic origin for the craters. The occurrence of sequential phreatomagmatic eruptions during the intrusion of the dykes may have been an important factor contributing to the prevention of magma eruption at surface and hence promoted long-range lateral propagation.

ACKNOWLEDGEMENTS

We are grateful to Schlumberger for an academic licence of Petrel. The paper contains information provided by the Oil and Gas Authority and/or other third parties. We thank the Editor, Chris Okubo and two reviewers for constructive comments.

REFERENCES

Bosworth, W., Stockli, D.F. and Helgeson, D.E., 2015. Integrated outcrop, 3D seismic, and geochronologic interpretation of Red Sea dike-related deformation in the Western Desert, Egypt–the role of the 23 Ma Cairo “mini-plume”. *Journal of African Earth Sciences*, *109*, pp.107-119. https://doi.org/10.1016/j.jafrearsci.2015.05.005

Brown, G., Platt, N.H., and McGrandle, A. 1994. The geophysical expression of Tertiary dykes in the southern North Sea. *First Break*, 12, 137-146. https://doi.org/10.3997/1365-2397.1994011

Carver, F., Cartwright, J., McGrandle, A., Kirkham, C. and Pryce, E., 2023. The continuation of the Mull Dyke Swarm into the Southern North Sea. *Journal of the Geological Society*, *180*, https://doi.org/10.1144/jgs2023-039.

Delaney, P.T. 1982. Rapid intrusion of magma into wet rock: Groundwater flow due to pore pressure increases. *Journal of Geophysical Research,* 87, 7739-7756. https://doi.org/10.1029/JB087iB09p07739

Ernst, R.E., Head, J.W., Parfitt, E., Grosfils, E. and Wilson, L., 1995. Giant radiating dyke swarms on Earth and Venus. *Earth-Science Reviews*, *39*(1-2), pp.1-58. https://doi.org/10.1016/0012-8252(95)00017-5

Fialko, Y.A. and Rubin, A.M., 1999. Thermal and mechanical aspects of magma emplacement in giant dike swarms. *Journal of Geophysical Research: Solid Earth*, *104*(B10), pp.23033-23049.

https://doi.org/10.1029/1999JB900213

Gradstein, F., Ogg, J.G., Schmitz, M.D. and Ogg, G.M. eds., 2012. *The Geologic Time Scale 2012*. Elsevier.

Head, J.W., Crumpler, L.S., Aubele, J.C., Guest, J.E. and Saunders, R.S., 1992. Venus volcanism: Classification of volcanic features and structures, associations, and global distribution from Magellan data. *Journal of Geophysical Research: Planets*, *97*(E8), pp.13153-13197. https://doi.org/10.1029/92JE01273.

Lister, J.R. and Kerr, R.C., 1991. Fluid-mechanical models of crack propagation and their application to magma transport in dykes. *Journal of Geophysical Research: Solid Earth*, *96*(B6), pp.10049-10077. https://doi.org/10.1029/91JB00600.

Lott, G.K. and Knox, R.W.O'B. 1994. Post-Triassic of the southern North Sea. *In:* Knox, R.W.O'B. & Cordey, W.G. (eds) *Lithostratigraphic Nomenclature of the UK North Sea*. British Geological Society, Keyworth, Nottingham, 7. 155.

Lorenz, V., 1986. On the growth of maars and diatremes and its relevance to the formation of tuff rings. *Bulletin of volcanology*, *48*, 265-274. https://doi.org/10.1007/BF01081755

Lorenz, V., 2003. Maar-diatreme volcanoes, their formation, and their setting in hard-rock or soft-rock environments. *Geolines*, *15*, pp.72-83.

Macdonald, R., Wilson, L., Thorpe, R.S. and Martin, A., 1988. Emplacement of the Cleveland dyke: evidence from geochemistry, mineralogy, and physical modelling. *Journal of Petrology*, *29*(3), pp.559-583. https://doi.org/10.1093/petrology/29.3.559

Magee, C., Ernst, R.E., Muirhead, J., Phillips, T., Jackson, C.AL. (2019). Magma Transport Pathways in Large Igneous Provinces: Lessons from Combining Field Observations and Seismic Reflection Data. In: Srivastava, R., Ernst, R., Peng, P. (eds) *Dyke Swarms of the World: A Modern Perspective.* Springer Geology. Springer, Singapore. https://doi.org/10.1007/978-981-13-1666-1_2

Magee, C., Kling, C., Byrne, P. and Jackson, C.L., 2022. Seismic reflection data reveal the 3D subsurface structure of pit craters. *Journal of Geophysical Research: Planets*, 127, e2021JE007155. https://doi.org/10.1029/2021JE007155

Mège, D. and Masson, P., 1996. Amounts of crustal stretching in Valles Marineris, Mars. *Planetary and Space Science*, *44*(8), 749-781. https://doi.org/10.1016/0032-0633(96)00013-X

Morton, A.C. and Knox, R.O.B., 1990. Geochemistry of late Palaeocene and early Eocene tephras from the North Sea Basin. *Journal of the Geological Society*, *147*(3), pp.425-437. https://doi.org/10.1144/gsjgs.147.3.0425

Okubo, C.H. and Martel, S.J., 1998. Pit crater formation on Kilauea volcano, Hawaii. *Journal of Volcanology and Geothermal Research*, *86*(1-4), pp.1-18. https://doi.org/10.1016/S0377-0273(98)00070-5

Parfitt, E.A. and Head III, J.W., 1993. Buffered and unbuffered dike emplacement on Earth and Venus: implications for magma reservoir size, depth, and rate of magma replenishment. *Earth, Moon, and Planets*, *61*(3), pp.249-281. https://doi.org/10.1007/BF00572247

Rivalta, E., Taisne, B., Bunger, A.P. and Katz, R.F., 2015. A review of mechanical models of dike propagation: Schools of thought, results and future directions. *Tectonophysics*, *638*, pp.1-42. https://doi.org/10.1016/j.tecto.2014.10.003

Scott, E. D., and Wilson, L., 2002, Plinian eruptions and passive collapse events as mechanisms of formation for Martian pit chain craters: *Journal of Geophysical Research: Planets,* 107, 4-1-4-11. https://doi.org/10.1029/2000JE001432

Scott, E.D., Wilson, L. and Head III, J.W., 2002. Emplacement of giant radial dikes in the northern Tharsis region of Mars. *Journal of Geophysical Research: Planets*, *107*(E4), pp.3-1. https://doi.org/10.1029/2000JE001431

Stokke, E.W., Liu, E.J. and Jones, M.T., 2020. Evidence of explosive hydromagmatic eruptions during the emplacement of the North Atlantic Igneous Province. *Volcanica*, *3*(2), pp.227-250. https://doi.org/10.30909/vol.03.02.227250

Underhill, J.R., 2009. Role of intrusion-induced salt mobility in controlling the formation of the enigmatic 'Silverpit Crater', UK Southern North Sea. *Petroleum Geoscience,* 15, 197-216. https://doi.org/10.1144/1354-079309-843

Wall, M., Cartwright, J., Davies, R. and McGrandle, A., 2010. 3D seismic imaging of a Tertiary Dyke Swarm in the Southern North Sea, UK. *Basin Research*, 22, 181-194. https://doi.org/10.1111/j.1365-2117.2009.00416.x

Wyrick, D., Ferrill, D.A., Morris, A.P., Colton, S.L. and Sims, D.W., 2004. Distribution, morphology, and origins of Martian pit crater chains. *Journal of Geophysical Research: Planets*, *109* (E06005) doi:10.1029/2004JE002240.

Figure Captions

Figure 1: (A) The Mull Dyke Swarm (after Carver et al. 2023) originating on the Isle of Mull (M), crossing the Highland Boundary Fault (HBF), Southern Uplands Fault (SUF) and Iapetus Suture Zone (ISZ). (B) Focus area and outline of the 3D seismic survey used to map Dykes A, B &C. Figure locations indicated. Wells: A- 44/11-3, B- 44/23a-12, C- 44/23-4, D- 44/29b-4.

Figure 2: A: Representative seismic expression of one of the major dykes (Dyke B), showing the dyke obscured by a SDZ (see text). Crater geometry clearly imaged at the top of the SDZ. **B:** Crater trail of crater array associated with Dyke B as mapped at Top Chalk (TC). BCU – Base Cretaceous Unconformity. Location in Fig. 1B.

Figure 3: Well calibration of a crater fill and crater flank anomaly. A: Well 44/11-3 has a trajectory through the axis of a large crater associated with Dyke A. Data insets from the well reports. B: Well 44/29b-4 calibrates the crater flank anomaly and is associated with Dyke C. The anomaly comprises two thin reworked chalk layers interbedded with Palaeocene mudstones. Location in Fig. 1B.

Figure 4: Model of pit crater formation by phreatomagmatic eruption via vertical conduit above dyke tip during shallow-level dyke intrusion (after Lorenz, 1986).

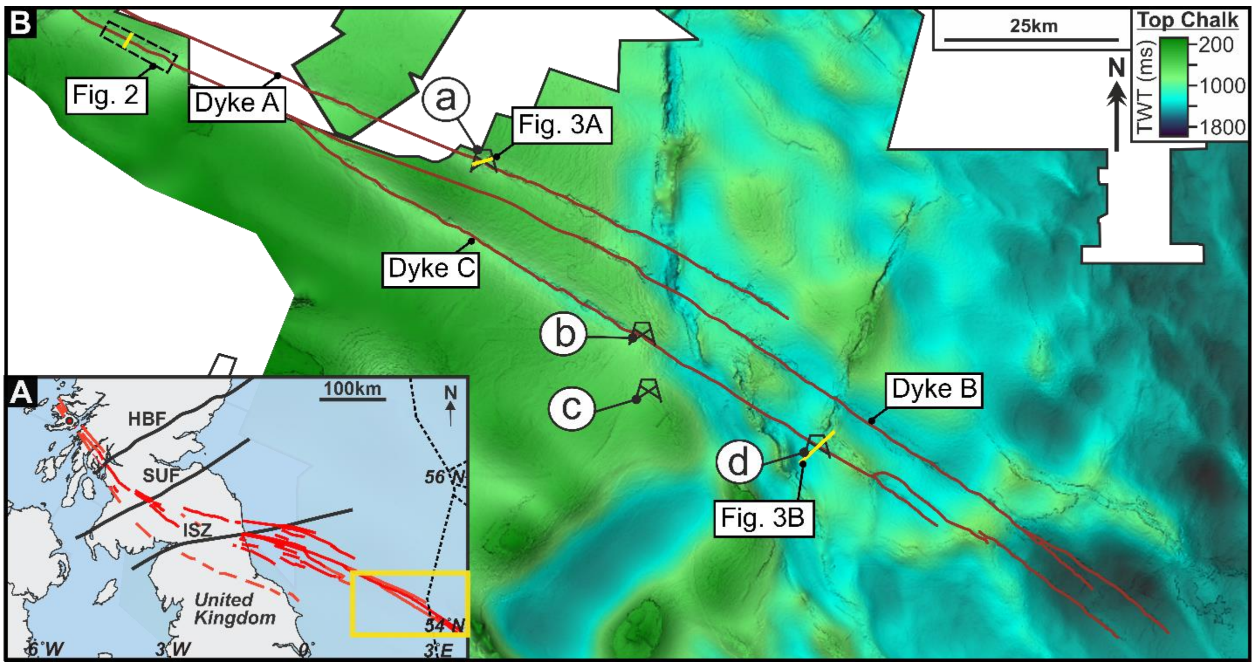

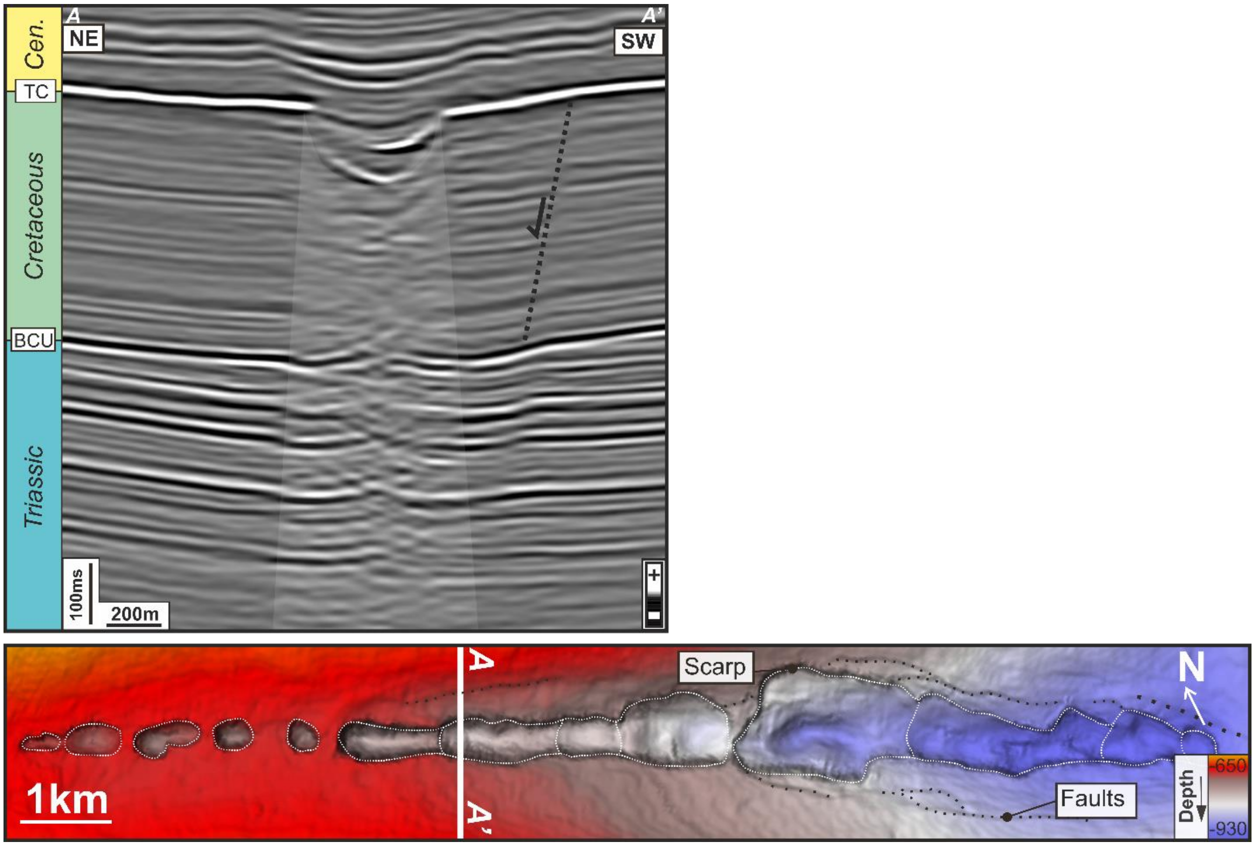
A
A'
NE
SW
Cen.
TC
Cretaceous
BCU
Triassic
100ms
200m
+
-
A
A'
Scarp
N
-650
Depth
-930
Faults
1km

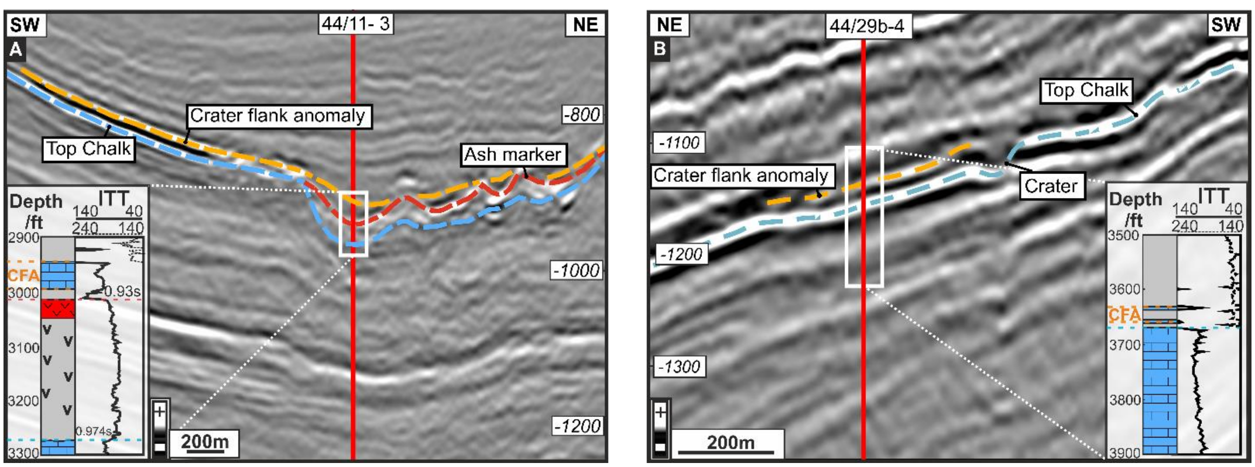
SW
44/11- 3
NE
A
Crater flank anomaly
-800
Top Chalk
Ash marker
Depth /ft
ITT
140 40
240 140
2900
CFA
3000
0.93s
3100
3200
0.974s
3300
-1000
-1200
200m
NE
44/29b-4
SW
B
Top Chalk
-1100
Crater flank anomaly
Crater
-1200
Depth /ft
ITT
140 40
240 140
3500
3600
CFA
3700
-1300
3800
200m
3900

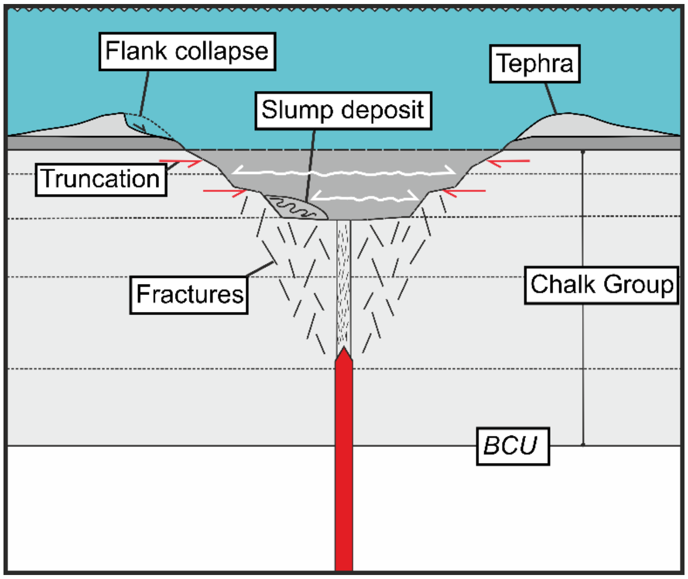
Flank collapse
Tephra
Slump deposit
Truncation
Fractures
Chalk Group
BCU

GSA DATA REPOSITORY

Supplemental material for

"Sequential phreatomagmatic eruptions during long-range lateral propagation of a giant dyke swarm"

Evan Pryce, Joe Cartwright, Chris Kirkham and Dan Phillips

Department of Earth Sciences, University of Oxford, South Parks Road, Oxford OX1 3AN, UK

Database

A combination of seismic, well-log and aeromagnetic data was used to identify the dykes and interpret the detailed seismic expression of their upper tip regions and associated pit craters in the Southern North Sea (Fig. S1). The primary dataset for the bulk of the mapping consisted of the Southern North Sea 3D seismic megamerge (processed by PGS UK Ltd and released under academic licence from the North Sea Transition Authority (NSTA)), an amalgamation of individual 3D surveys with different acquisition histories, dating back to 1998 (Fig. S2). Each survey was acquired by air gun and streamer, covering an extent of 65,632km^2 of the Southern North Sea over territorial waters of the UK and the Netherlands. The seismic volume consisted of inlines at a bearing of 130NW, crosslines at 045NE spaced at 25m by 25m, processed to generally zero phase and displayed with a positive polarity (positive acoustic impedance contrasts are displayed as positive amplitude values).

The resolution of the seismic data across the megamerge is variable because the processing parameters, including the dominant frequency, are individual to each component survey. The typical vertical resolution (limit of separability) in the post-Zechstein interval is of the order of 15-30m based on a typical dominant frequency of 25-30Hz and an interval velocity that varies from c.2000- c.3000m/s. Lateral resolution is approximated by the bin size of 25m (Brown, 2011).

An additional 3D survey, the Cavendish survey, was used to fill the major gap in the PGS megamerge in Quadrant 43 (Fig. S2), and has similar polarity and resolution limits (both vertically and laterally) to the megamerge survey.

Hundreds of released petroleum exploration boreholes (archived by the NSTA) provided calibration of the seismic data, and gave local velocity control for depth conversion of the seismic data. Data extracted from the archive included completion logs, petrophysical logs (particularly Gamma Ray, Resistivity, Sonic Velocity and Density). Well to seismic ties were undertaken using depth to time calibration exclusively derived from Vertical Seismic Profiles downloaded from the NSTA archive. Errors in tying specific lithological boundaries to seismic marker horizons are estimated at +/- 20m (arising due to shifts in the input data, and interpretative error), which typically corresponds to half a seismic wavelength in the interval of interest.

Background on use of the term Pit Crater Chain

Pit Crater Chains (PCCs) are linearly aligned trails of small depressions identified on Earth, Venus, Mars and other planetary bodies (Wyrick and Buczkowski, 2022). Originally, the term was applied to a specific type of crater observed above shallow concealed tips of dykes that were interpreted to form by collapse above fractures related to dyke emplacement (Okubo and Martel, 1998; and references therein).

Numerous studies have argued that they form above concealed shallow level dykes (e.g. Mège and Masson, 1996; Okubo and Martel, 1998; Scott and Wilson; 2002; Magee et al., 2017), and this link between dyke intrusion and the formation of PCCs has been instrumental in the interpretation of giant dyke swarms on Venus and Mars (Ernst et al. 1995; Scott and Wilson, 2002). However, other studies have argued that the formation of PCCs is instead the result of collapse into subsurface voids produced by dilational faulting (e.g. Wyrick et al. 2004; Ferrill et al. 2011; Wyrick and Buczkowski, 2022), casting doubt on their unequivocal use to guide shallow dyke interpretations.

Seismic Interpretation and Mapping

The main focus of this study was to map pit craters associated with dykes mapped previously by Carver et al. (2023) and linked to the MDS. Prior to mapping dykes and associated pit craters, key horizons were interpreted regionally and calibrated with industry boreholes. Top and Base Chalk (corresponding to Top Cretaceous and Base Cenomanian) were mapped throughout the study area, along with the Base Zechstein (Late Permian) (Fig. 3), using the Petrel seismic interpretation package of Schlumberger. The Top Chalk marker is found to be an unconformity in wells across the study area, with the Late Palaeocene claystones generally found juxtaposed with Late Maastrichtian chalks (c.f. Wall et al. 2010).

We identified dykes in profile on the megamerge 3D survey from their characteristic sub-vertical zones of reduced seismic coherence or seismic disturbance zones (SDZs) (Underhill, 2009; Wall et al. 2010; Carver et al. 2023) (Figs. S1, S3). The dykes themselves are not imaged but diffractions, reflected refractions, attenuation due to scattering, and large and abrupt lateral velocity contrasts combine to produce the zone of 'seismic disturbance' of much wider extent than the dykes themselves (Figs. 2, S1, S3) (c.f. Magee et al, 2022). Upper tip positions of dykes cannot be identified directly from the seismic data, only inferred from their effects on the host sediments. Where dykes are not vertical, it is often possible to interpret a much narrower zone of disturbance or loss of reflection coherence that more closely defines the dyke trajectory through a reflective sedimentary succession (c.f. Wall et al. 2010).

Over the full extent of the 3D seismic coverage, dykes identified from profiles using these criteria corresponded to significant disruption of the Top Chalk horizon as has been noted previously by Brown et al. (1994) and Wall et al. (2010)(Fig. 2, S1, S3). Dyke trajectories could be quickly identified by mapping the Top Chalk, and validated using profile-based criteria or time slice interpretation of the coherency volumes extracted from the 3D seismic data.

Interpretation of pit craters

Initial identification of craters was based on detailed mapping of the Top Chalk marker horizon. Manually picked grids of inlines and crosslines spaced at 100m were used as a basis for autotracking, and any poor quality picks were manually edited. Well to seismic tie of the key calibration well of 44/11-3 was used for the crater fill and crater base interpretation (Fig. 3A, Fig. S8), and the seismic response of the crater base and fill was used to inform the manual picking of crater bases along the remainder of the pit crater chains. Crater bases were invariably found to coincide with significant amplitude anomalies, and the bases were consistently picked at the base of these anomalies based on the 44/11-3 experience. Crater margins were picked carefully to highlight the surface morphology, which in many cases was found to be irregular, with evidence for retrogressive failure of crater sidewalls (Fig. S3). Point locations were assigned to the deepest part of all crater bases. Measurements of diameter were made on short and long axes of the generally elliptical depressions (Fig. S5). Errors in diameter measurements are estimated to be <25m, corresponding to twice the bin size. Relief was measured from the intact shoulders at Top Chalk to the deepest point of the crater base. Errors in the crater relief measurements are considered to be < 40m based on the typical uncertainty in lateral correlation of crater bases.

Other tip structures including dyke-related faults

Other features of note in the upper tip regions of the dykes were interpreted in detail (e.g. Fig. S3) (Pryce, 2023). These included full grabens or single normal faults that could be classified as dyke-related (c.f. Magee et al. 2022). The types of upper tip structures were recorded at 250m intervals along the strike of the major dyke in the central group but no systematic relationships could be discerned from their distribution (Pryce, 2023).

Brown, A.R., 2011. *Interpretation of three-dimensional seismic data*. Society of Exploration Geophysicists and American Association of Petroleum Geologists.

Pryce, E. 2023. Upper tip structures of the Mull Dyke Swarm, southern North Sea, MESci thesis, University of Oxford. pp78.

Wyrick, D.Y. and Buczkowski, D.L., 2022. Pit crater chains across the solar system: evidence for subterranean tectonic caves, porosity and permeability pathways on planetary bodies. *Journal of Geophysical Research: Planets*, *127*(12), p.e2022JE007281.

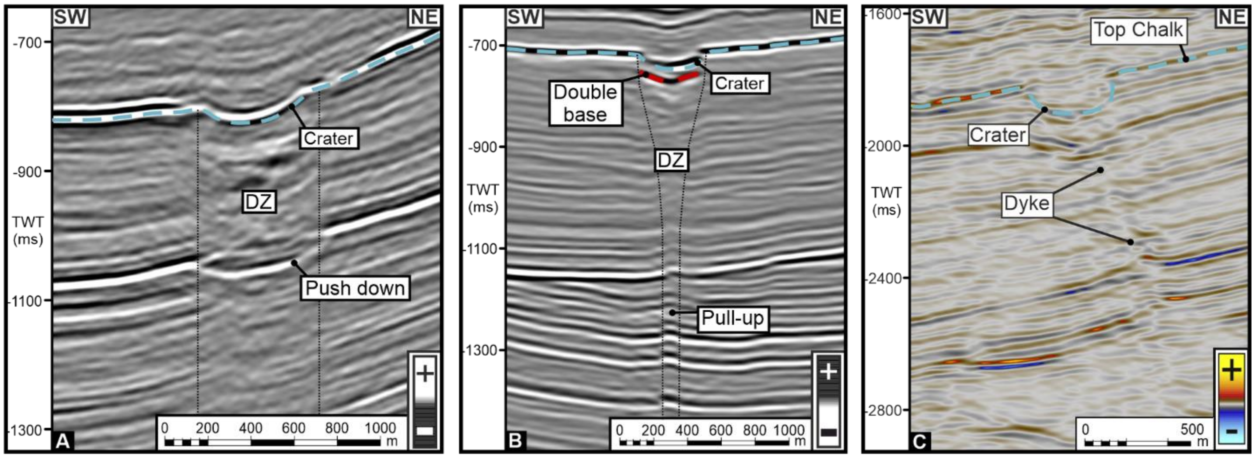

Figure S1: **A** representative selection of examples of seismic profiles extracted from the megamerge survey across different dykes within the Mull Dyke Swarm. These show the variety of seismic expression of SDZs and the variation in image quality between the component surveys of the merged data volume. In A and B, the position of the dyke is impossible to discern due to the broader zone of seismic artefacts, but in C, the dyke position is quite narrowly defined because the dyke itself is steeply dipping, and this allows discontinuities due to dyke intrusion to be differentiated from dominantly vertical artefacts arising from the crater in the uppermost Chalk.

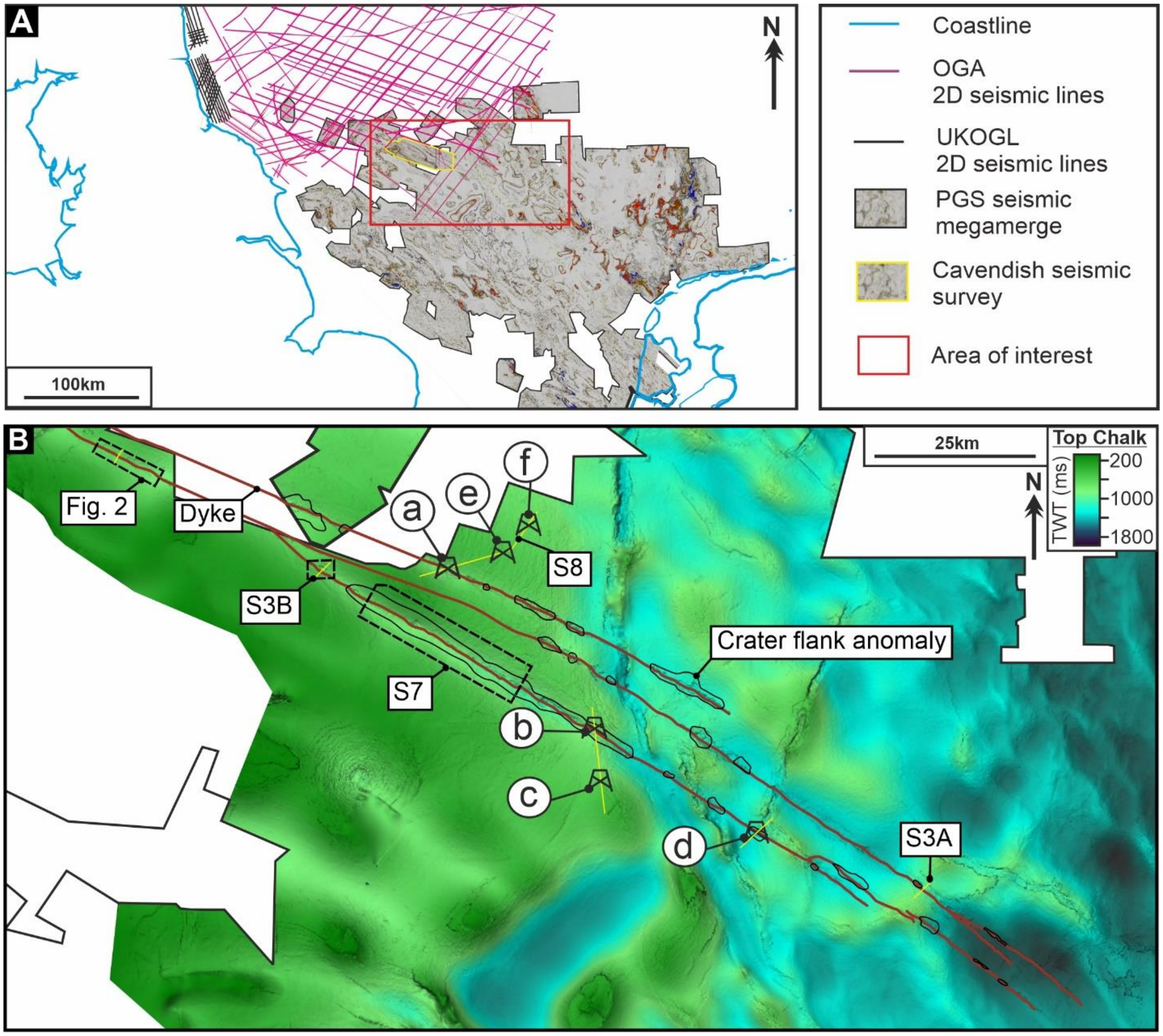

Figure S2. A: Database of 2D and 3D reflection seismic surveys used in this study, with outline of area of interest. B: Time structure map of the Top Chalk over the area of interest based on mapping using the megamerge 3D seismic survey showing locations of figures in the Data Repository, outlines of the crater flank anomalies, and positions of wells referred to in the text and Supplementary Information (A- 44/11-3, B- 44/23a-12, C- 44/23-4, D- 44/29b-4, E- 44/11-2, F- 44/11a-4).

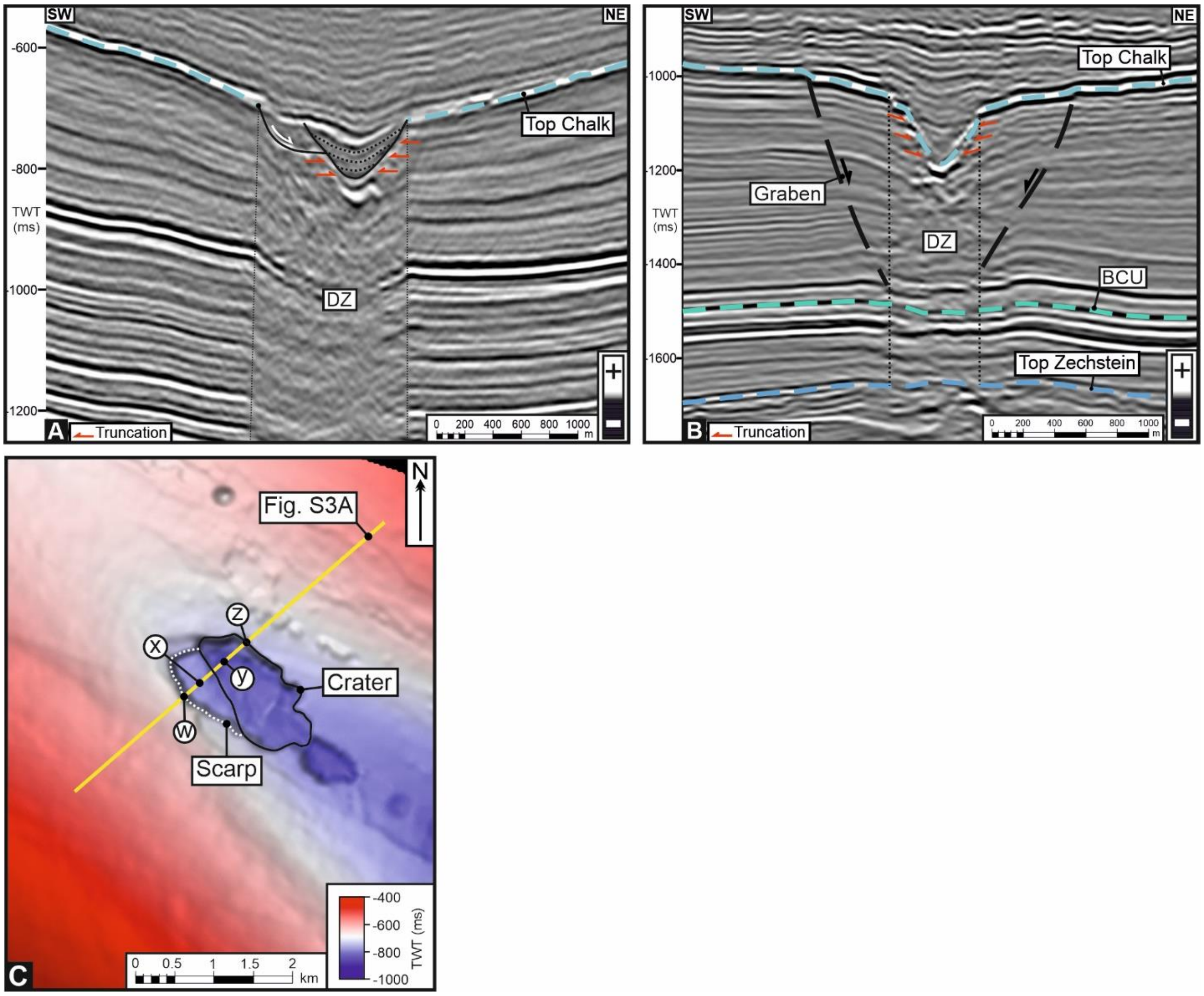

Figure S3. Seismic profiles showing seismic expression of the crater morphology. A: Profile across a crater which exhibits enlargement through flank collapse. B: profile across a well- defined crater, with clear erosional truncations and onlap fill. Note the occurrence of normal faults dipping inwards symmetrically disposed on the flanks of the SDZ and bisecting the position of the crater (see for comparison Magee et al. (2022). These faults tip upwards close to the Top Chalk, but their basal tips are difficult to interpret, and either occur at or below the Base Cretaceous Unconformity (BCU). C: Top Chalk map of the crater shown in A with location of the profile shown in yellow, and points annotated W-Z. The arcuate scarp (dotted black line) is the failure surface shown in A, interpreted to result from late collapse into the initial crater (solid black line).

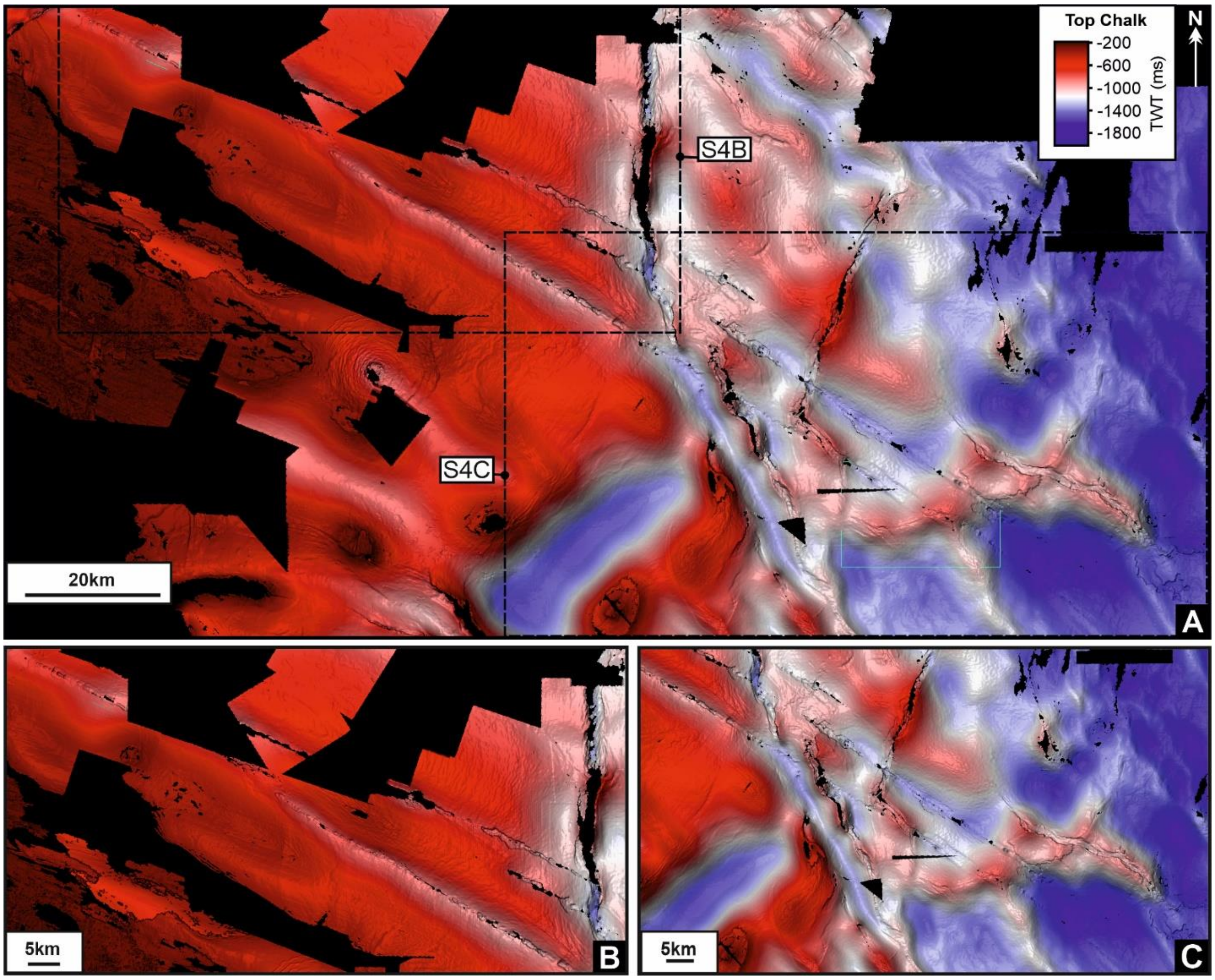

Figure S4: Time structure maps of the Top Chalk over the entire area of interest (A), with details of sub areas shown in B and C. The pit crater chains can be seen clearly associated with the three main dykes of the central part of the Mull Dyke Swarm (see also Carver et al. 2023).

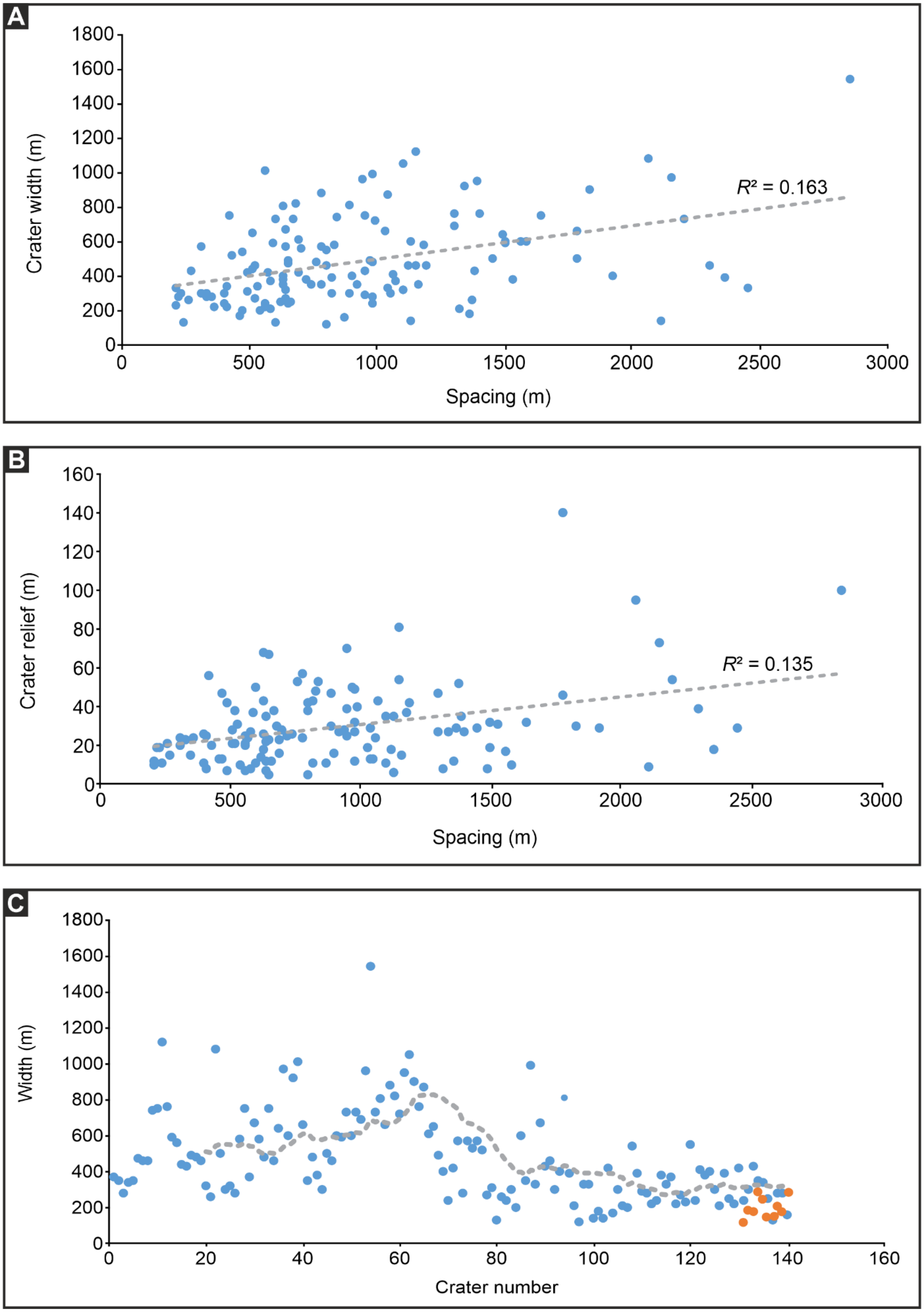
A
Crater width (m)
Spacing (m)
R^2 = 0.163
B
Crater relief (m)
Spacing (m)
R^2 = 0.135
C
Width (m)
Crater number

Figure S5: Morphometric data for craters from Dykes B (red points) and C (blue points) showing no significant correlation between crater width (A) or relief (B) and the spacing between craters. There is a modest indication of a reduction in crater width in the propagation direction, more noticeable towards the distal, SE tip region (dashed grey line is a running mean value binned by 10 craters).

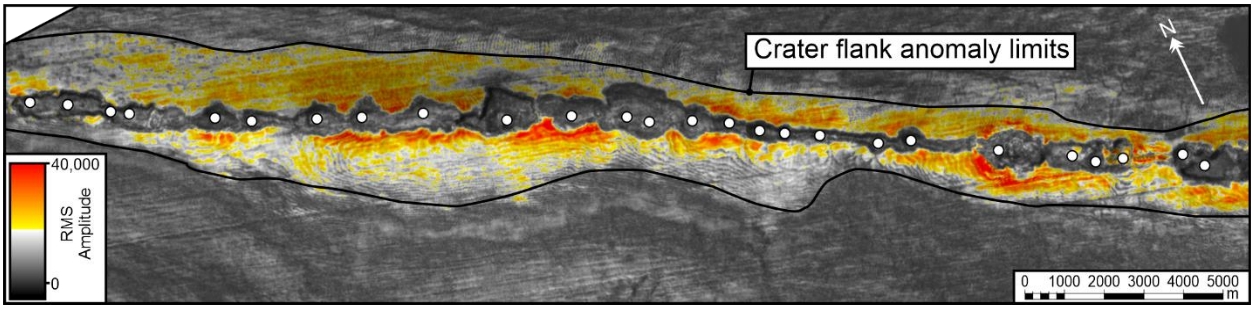

Figure S6: Crater flank seismic anomaly for Dyke C (location in Fig. S2), based on a root mean squared (RMS) amplitude extraction from a horizon (orange marker in S7) mapped immediately above the Top Chalk marker. The amplitude anomaly is clearly limited to the immediate flanks of the craters associated with Dyke C. The highest amplitudes gradually decrease away from the craters to the North and South as the anomaly merges into the background amplitude value (grey tones).

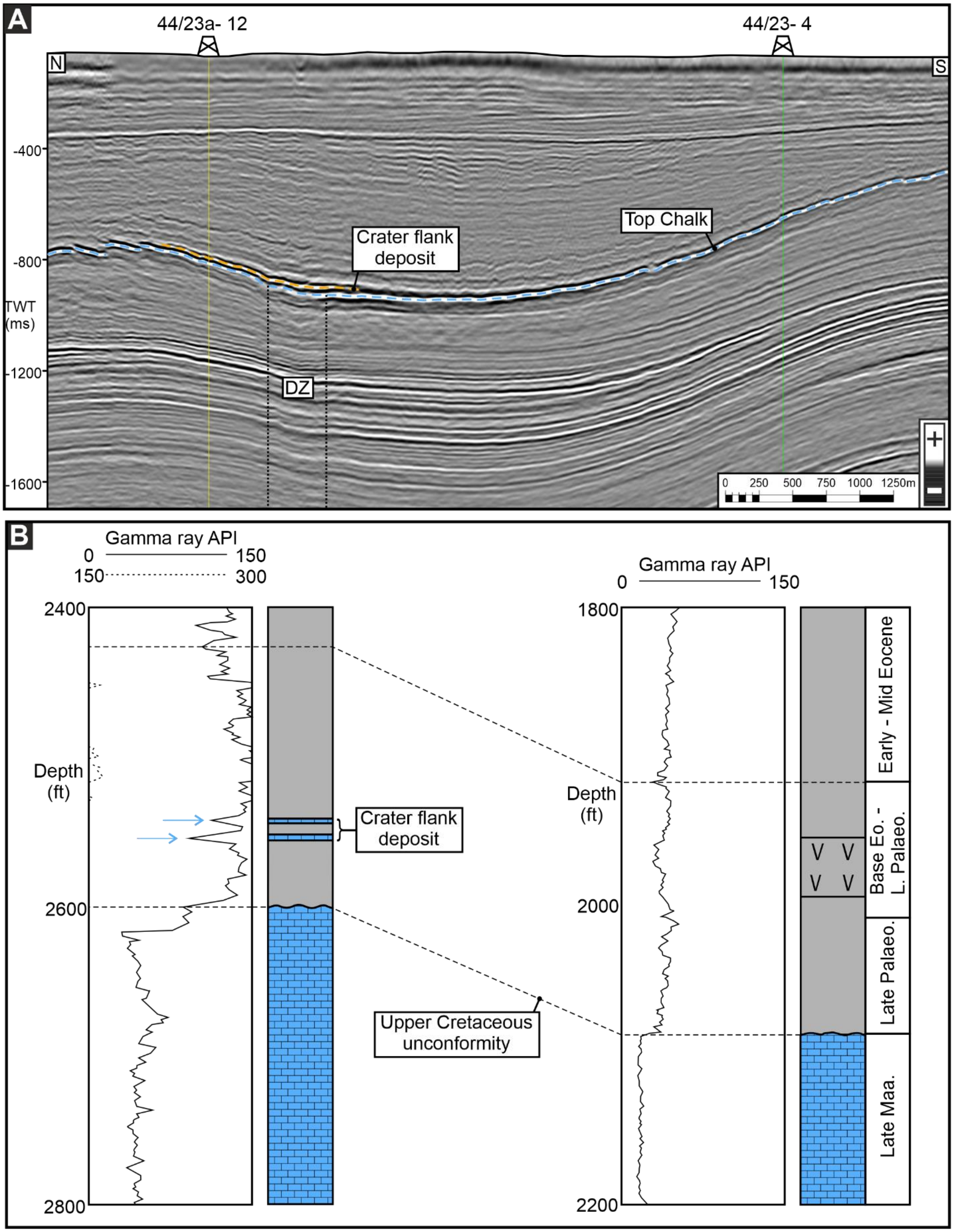

Figure S7: A- Seismic traverse between two key calibration wells, 44/23a-12 and 44/23-4 (location in Fig. S2). This profile shows the additional reflection (orange marker) immediately above the Top Chalk, restricted to a region flanking the SDZ. Note that the whole region has been folded subsequently to dyke intrusion, with a detachment within the Zechstein evaporites. B- the well correlation panel between 44/23a-12 and 44/23-4, showing the gamma ray spikes that correlate with reworked chalky sediments (with Late Cretaceous microfossils) in 44/23a-12 and that tie to the orange marker and the crater flank anomaly (of Fig. S6). Legend for lithologies is in Fig. S8.

518

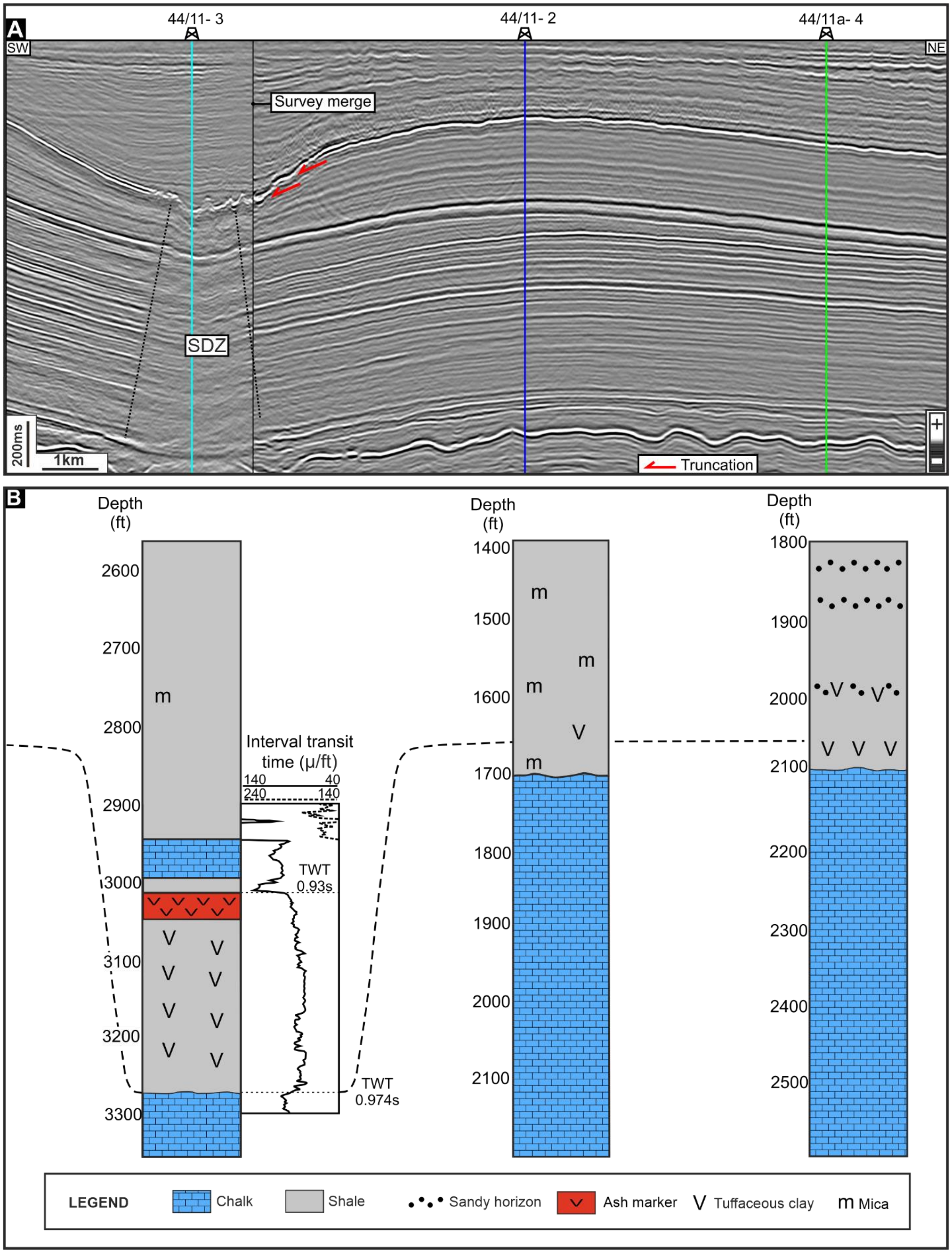

A
44/11- 3
44/11- 2
44/11a- 4
SW
NE
Survey merge
SDZ
200ms
1km
Truncation
B
Depth (ft)
2600
2700
2800
2900
3000
3100
3200
3300
m
V
Interval transit time (μ/ft)
140 40
240 140
TWT 0.93s
TWT 0.974s
1400
1500
1600
1700
1800
1900
2000
2100
2200
2300
2400
2500
LEGEND
Chalk
Shale
Sandy horizon
Ash marker
Tuffaceous clay
Mica

Figure S8. A- Seismic traverse between three key calibration wells showing the context for the important well 44/11-3 that was drilled through one of the pit craters associated with Dyke A (location in Fig. S2). The traverse crosses the locations for two wells drilled away from the flanks of the crater chain, namely 44/11-2, and 44/11a-4. These two wells penetrated a stratigraphically complete Late Cretaceous succession (Chalk Group), whereas correlation to 44/11-3 shows that >200m of uppermost Chalk Group is missing from that well. B- Well summary information for the correlation panel for these three wells in A, with simplified lithologies from the completion reports, and a short segment of sonic log to show the well ties to the key markers. The 44/11-3 well calibrates the crater fill with the ash marker prominent within the crater fill, set within a tuffaceous mudstone unit that differs considerably from the Late Palaeocene succession in the two flank wells. Reworked chalky sediments are also evident as part of the crater fill. The base of the crater is picked at the erosional contact between in situ Chalk and overlying tuffaceous mudstone (dashed line). Values in two-way travel time (TWT) are given for the two key markers (Ash Marker, and Crater Base).